Modeling Pedestrian Mobility in Disaster Areas

Gürkan Solmaz[a,b], Damla Turgut[b]
[a]NEC Laboratories Europe, Heidelberg, Germany
Email: gurkan.solmaz@neclab.eu,
[b]Dept. of Computer Science, University of Central Florida, Orlando, USA
Email: turgut@eecs.ucf.edu

***Abstract*—Realistic mobility modeling is necessary for testing disaster management strategies as well as performance of disaster-resilient networks. Evacuation of the people from a disaster area depends on the environment and type of the hazard which cause certain changes in the pedestrian flows. Although most models focus on the building evacuations or city-scale evacuation planning, there is a need for a mobility model that captures the pedestrians' movement behavior during evacuation from large and crowded disaster areas such as theme parks.**

In this paper, we propose a mobility model of the pedestrians in disaster areas. In our application scenario of theme parks, the main mission of the operators is the evacuation of the visitors and providing access to transportation vehicles such as ambulances. We use real maps to generate theme park models with obstacles, roads, and disaster events. We incorporate macro and micro mobility decisions of the visitors, considering their local knowledge and the social interactions among the visitors. We analyze the outcomes of the simulation of our theme park disaster (TP-D) mobility model with simulations of currently used models and real-world GPS traces. Moreover, using the proposed model as a baseline, we analyze the performance of an opportunistic network application.

***Index Terms*—Mobility model, disaster resilience, wireless sensor networks, theme parks**

I. Introduction

Performance results of mobile networks drastically change with the mobility model used in the simulations [1]. Therefore, accurate modeling of mobility has utmost importance for realistic network simulations and performance evaluation of protocols [2]. With the increased popularity of smartphones and mobile applications, modeling human mobility has become a major area of interest for networking researchers. While there exist very limited publicly available GPS trace datasets, synthetic mobility models which simulate the human mobility are useful for evaluating performances of various network models including urban sensing networks and opportunistic social networks.

Human mobility is based on the combinations of many factors including deterministic and non-deterministic decisions and social factors which depend on the scenario. Since generic human mobility models are not suitable to represent the human mobility behavior in different application scenarios, there is a need for scenario-specific modeling. We consider the application scenario of theme parks due to their certain characteristics such as allowing limited use of vehicles, having large-scale areas and including natural and man-made obstacles. Moreover, theme parks have similarities to other environments with limited vehicle use such as campus environments, airports, shopping malls, state fairs, and so on. By selecting theme parks as an application scenario, we isolate the problem of modeling pedestrian mobility from problems of vehicle mobility and mobility during building evacuations.

Theme parks are large and crowded areas with thousands of daily visitors. Particularly, large-scale theme parks attract visitors from all over the world, and the theme park industry is one of the main contributors of their regions. While overall popularity of theme parks and the size of the industry are growing every year, the global success of theme parks is severely affected by disasters such as Hurricane Irene [3]. Considering the fact that climate change increases the risk of extreme events such as forest fires and floods [4], effect of disasters may cause damages to the regions such as Central Florida. This region has 5 of the top-10 theme parks with highest attendances in the world, while being home to various natural disasters with a history of hurricanes, floods, tornadoes, and tropical storms.

The studies on disaster recovery and opportunistic communication networks have become major research interests due to their prospective contributions on the disaster management strategies. For instance, as an impact of a disaster, communication infrastructures which are pre-deployed in the area may become unoperational. For this reason, communication systems independent from the infrastructurens (e.g., [5]) are taken into account in

many disaster management studies. Crowd management and evacuation of people from disaster areas are other major challenges which have theoretical and practical interests from the research community. Modeling disaster mobility in theme parks is useful for finding novel methods to solve the evacuation problem in theme parks. In addition, these methods may become the base-case for the evacuation problem of more complicated scenarios such as evacuation of people from buildings and evacuation from big cities.

We consider a wide range of disaster scenarios for theme parks. These scenarios include natural disasters such as tornado, thunderstorm, hurricane, and earthquake. We also consider man-made disaster scenarios such as terrorist attacks which may threaten human lives in crowded places. While effects of these various types of disaster may differ from one another, the main goal of the operators will be safe and quick evacuation of visitors and providing them access to transportation vehicles.

We modeled visitor movements in theme parks to represent daily routine mobility of theme park visitors without any consideration of the disaster scenarios [6]. However, in our previous model and the other currently used theme park mobility models, the movement decisions of the visitors are based on visiting the attractions and exploring the park. Considering disaster scenarios, the movement decisions should be based on the security of visitors. The main goal of the theme park operation include finding easy ways to secure places and quickly evacuating the visitors from the disaster areas.

In this paper, we extend our previous work ([7], [8]) on disaster mobility in theme parks. The main contributions of this work include adding visibility variable to model, extending the model description and simulation study and evaluating the performance of an opportunistic communication network application based on our mobility model.

We model theme park as a combination of roads, obstacles, lands, and red-zones using real theme park maps. To model the visitor movements, we consider the macro and micro mobility decision problems separately. We use the social force model [9] to represent the dynamics of the human motion by the social interactions. We analyze the simulation results of our model and compare it with the currently used mobility models and the GPS traces collected from theme park visitors. The outcomes of the simulation of the proposed model are mobility traces of theme park visitors.

The effects of various possible disaster response approaches can be tested using our mobility model. Placing informative signs in strategic locations to direct the visitors to desired regions, having trained security personnel to manage crowd flows or forming visitor groups by assigning one trained person to lead each group can be considered as examples of disaster response strategies. Furthermore, autonomous robots can be used for missions such as search and rescue. Another use of our model is evaluating performances of networks resilient to disasters such as opportunistic social networks which are formed for broadcasting messages and increasing knowledge of the visitors.

The organization of the remaining of the paper is as follows. We describe the model in detail in Section II. The simulation results of our model are provided in Section III. We discuss the recent literature in mobility models, disaster mobility and disaster management approaches in Section IV and finally conclude in Section V.

II. Mobility Model

In this section, we present the human mobility model in theme parks for disaster scenarios. Let us first describe the characteristics of theme parks and creation process of the theme park models. Later, we will describe the mobility of the visitors in detail.

A. Characteristics of Theme Parks

To give a background on the problem, we first describe the fundamental characteristics of theme parks by looking from the mobility modeling perspective. Theme parks consist of attractions which are entertainment places including rides, restaurants, and places for other activities. Attractions consist of man-made structures (i.e. buildings) and they are connected to each other by roads (i.e. pedestrian ways). The roads also connect the entrance and exit points of the theme park with the attractions. They are usually used only by pedestrians, specific for theme park environment. Each road has a width which determines the capacity of the road for pedestrian flows. For instance, if a road is narrow and there are many people, the density of the people becomes large and as a result people cannot move fast enough on the road.

Theme parks are open-air areas but can also have buildings such as indoor rides, restaurants and gift shops. The area of theme parks include many physical obstacles for pedestrians. The physical obstacles include man-made and natural obstacles. People who spend their day in theme parks have activities such as visiting rides, walking among the attractions along the roads, and eating at the restaurants.

Due to the nature of the large and crowded area, a natural or man-made disaster may have devastating effects. As a disaster response strategy, in time of a

disaster, the aim is secure and fast evacuation the visitors from the theme park. Considering an example of tornado alert in a crowded day, the visitors should leave the park to reach the transportation services located outside the park. Since there are thousands of people leaving the park, the mobility of a single pedestrian cannot be considered independent from others. As a result, the social interactions between the pedestrians, which may cause slowdowns in pedestrian flows, should be considered for realistic mobility modeling.

The evacuation problem of theme parks is different from other evacuation problems. For instance, in a city scenario, the main purpose is a quick evacuation of the city through the effective share of streets by cars and public transportation services. Other types of evacuation scenarios focus on indoor evacuation, such as evacuation from buildings or from rooms of a building. On the other hand, the evacuation problem of theme parks includes large areas with physical obstacles and large numbers of pedestrians. As expected, the mobility of pedestrians during disasters has many differences compared with the typical mobility of people. Because of the aforementioned characteristics, theme parks require scenario-specific mobility modeling for evaluating performance of networks in disaster situations as well as simulating and testing various evacuation strategies.

B. Theme park models

We model the theme park as the combination of roads, obstacles, lands, and disaster events. Each road contains a set of waypoints, which are the movement points for the theme park visitors. In this case, length of a road is equal to the sum of the distances between each pair of its consecutive waypoints. The roads direct the visitors to the target locations in the map. The gates are considered as the target locations and they are placed close to the borders of the park. The gates connect the theme park with the outside world and facilities such as transportation vehicles (i.e. cars, ambulances, fire engines).

As mentioned, attractions contain man-made buildings and other structures such as a roller-coaster. In the typical times, the aim of the visitors is to visit the attractions. For the disaster scenario in which the visitors should be evacuated from the disaster area as quickly as possible, we consider the buildings as the obstacles which prevent the free movement of the visitors. Furthermore, we model the man-made structures other than the buildings in the park such as fences and walls as the obstacles. There are also natural obstacles in the environment, such as lakes, trees, forest, river, and so on. We do not focus on the evacuation problem from the buildings and assume that visitors do not spend time in the attractions after having a disaster alert.

The areas which neither include the obstacles nor the roads are classified as the lands. The lands can be used by pedestrians but they are not preferred unless there are unexpected conditions on the available roads. For instance, when a road is unavailable due to an impact of the disaster event, the lands might be chosen instead. In some exceptional cases, lands provide shortcuts between the waypoints. Disaster areas are classified as the red-zones and represented by the circular areas reflecting the effects of the disaster. In a real scenario, one can think the red-zones as the events which damage roads or bridges, caused by an earth-quake, a hurricane, a fire, a terrorist attack and so on. The red-zones have radius values which specify the damaged areas and active times. If a red-zone is in its active time and it effects an area including some portions of a road, the road is assumed to be unavailable at that particular time.

The model of the theme park can be created synthetically or using real maps. We choose to use OpenStreetMap (OSM) [10] to extract the real theme park maps and parse the OSM data to generate the roads, the obstacles, the lands, and the gates. We collect the waypoints using the OSM data and connect the consecutive waypoints to create the roads. We assign width values to the roads according to their OSM types (footway, path, and pedestrian way). Fig. 1 displays example of the real map of the Magic Kingdom park from the Disney World in Orlando (left-side), and the processed version of the map including the waypoints, the roads, the gates, and the obstacles (right-side). In these figures, the small dots represent the waypoints, while the lines connecting the waypoints are the roads and the closed polygons are the obstacles. The model also include red-zones which are added to the model according to their active times; however, they are not included in this initial processing of the maps. The two gates can be seen as the two small thick lines close to each other. The generation of the theme park models are done computationally, but it is possible to create a non-existing theme park in design stage manually and create the theme park model in the same fashion.

C. Modeling mobility of the visitors

Mobility behavior of the visitors is mainly based on the environment (e.g., obstacles, roads) and the disaster effects. We assume that the visitors have local knowledge of their environments as opposed to having a global knowledge. The local knowledge of the visitors is determined by their vision. The visibility of the visitors

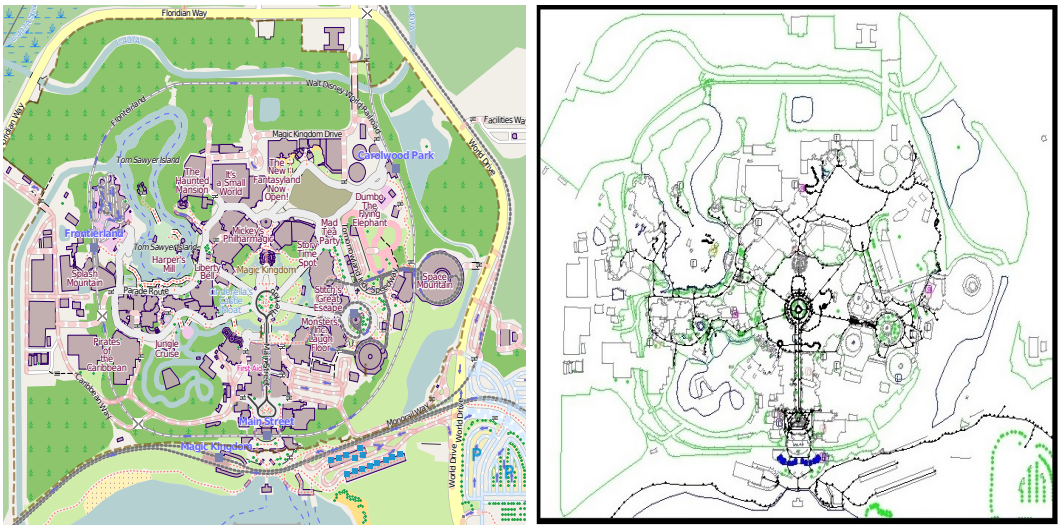

Fig. 1. The maps of the Magic Kingdom park. Left: the map extracted from (OSM), right: the processed map with 1300 waypoints.

may change as an effect of the disaster. The visitors are assumed not to communicate with each other and there is no broadcasting system for raising awareness.

Initially, the visitors are randomly distributed to one of the waypoints in the environment model. Each visitor selects an exit gate (the gate that the visitor already used to enter the area) and marks the gate's position as the target location (target point). A visitor is assumed as evacuated after reaching the target location. The visitor tries to reach the target point by moving among the waypoints. Whenever the visitor reaches a waypoint, marks it as visited. The next destination point is selected among all the visible waypoints. The visited waypoints, the waypoints positioned in a red-zone, or the waypoints that are not in the visible area are not taken into consideration as the candidates for the next destination point. The visitor selects the next destination point based on its distance and direction from the current position of the visitor. In other words, the selected destination point is the one closest to the target location among the candidates. The selection of the waypoints is constrained by the visitor's knowledge of the world, obstacles, and possible active red-zones along the way. Because of these constraints the visitor may not be able to find any candidate waypoint at certain times.

These are the times when the visitor does not see any visible movement location. In this case, we assume the visitor can shortly explore the surrounding to find new visible destinations. The exploration is made randomly by choosing a direction and a distance to move. The random exploration distance is a parameter that bounds the movement flexibility of the visitors in cases of the unexpected disaster events. Another parameter that effects the flexibility is the maximum visibility parameter. The visibility may differ based on the type and the impact of the disasters. Moreover, it may also differ during the disaster event by time and location of the visitor. The model produces random visibility with the upper bound of maximum possible visibility parameters throughout the simulation. It could also be possible to involve a more complex model to set the visibility parameter for each visitor based on their location and the time of the disaster (i.e., events happening at that time). In such a model, the factors such as the geographical features of the surroundings and the nature of different disasters should be taken into account.

We classify all the above steps of a visitor considering the global movement starting from the initial point to the target point as macro-mobility behavior of the visitors. The speeds of the visitors differ from one to another. Basically, each visitor has a maximum speed that depends on physical attributes of the individual such as age, gender, and weight. The speed of each individual is a random value between the global minimum and the global maximum speed of the visitors. The speed of a visitor varies from its minimum of 0 to maximum speed. On the other hand, the global minimum value determines the minimum value for the maximum speed value of all visitors. The maximum speed is the speed when the visitor is completely free to walk without disturbance or the obstacles. In the disaster scenario, the actual speed of a visitor is less than the maximum speed most of the times due to the effects of the social interactions which are explained below.

Fig. 2 illustrates the complete theme park model generated using the map of the Epcot park in Disney

vcentering 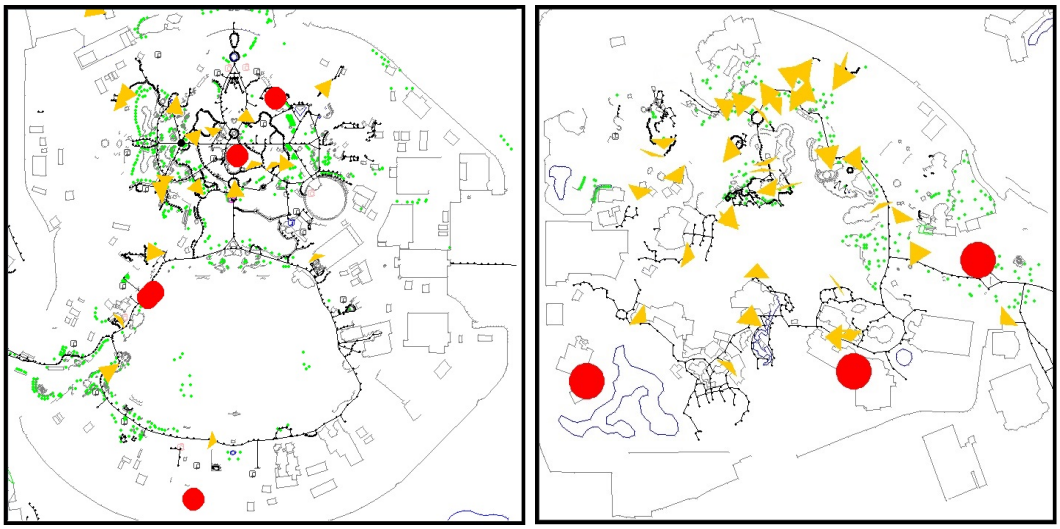

Fig. 2. Illustrations from the mobility model. Left: Epcot simulation with 20 visitors and 5 red-zones. Right: Islands of the adventure with 40 visitors and 3 red-zones.

World. In this figure, the visitors and the red-zones are included in the model. Twenty visitors moving on the roads are represented by the triangles. The shapes of the triangles illustrate the directions and velocities of each visitors. The red-zones are represented by the big circles. On the left figure, the two red-zones having an intersection area appeared as an enlarged red-zone, located in the middle of the figure.

We consider micro-mobility as the mobility of a visitor between the two consecutive waypoints separately from the macro-mobility model and the theme park model. We use the social force model (SFM) [9] which is used by the simulators such as SimWalk and VisSim for the micro-mobility. According to the social force concept, behavioral changes in the human motion can be explained and is actually caused by the combination of the social interactions. Using the SFM, we model the social forces on the visitors according to their social interactions with the environment. By this model, the visitors adapt their speed and direction of the movement from a waypoint to another. In SFM, the sum of the social forces is given by

$$f_\alpha(t) = \frac{1}{\tau_\alpha}(v_\alpha^0 e_\alpha^0 - v_\alpha) + \sum_{\beta(\neq\alpha)} f_{\alpha\beta}(t) + \sum_i f_{\alpha i}(t), \quad (1)$$

for a visitor α where τ_α denotes the relaxation time, $v_\alpha^0 e_\alpha^0$ is the desired velocity, and the sums correspond to the social forces by the other visitors (β) and the obstacles (i) respectively. The acceleration is then given by $f_\alpha(t)$ and the individual fluctuations. Assuming $f_{\alpha\beta}(t) = f(d_{\alpha\beta}(t))$, circular specification is given by

$$f(d_{\alpha\beta}) = A_\alpha e^{-d_{\alpha\beta}/B_\alpha} \frac{d_{\alpha\beta}}{\|d_{\alpha\beta}\|}, \quad (2)$$

where $d_{\alpha\beta}$ is the distance vector between α, β and A_α, B_α denote the interaction strength and the interaction range respectively.

For the elliptical specification of the model, the circular specification formula is expressed as a gradient of an exponential decaying potential $V_{\alpha\beta}$, where elliptical interaction force via the potential is $V_{\alpha\beta}(b_{\alpha\beta}) = ABe^{-b_{\alpha\beta}/B}$. In this equation, $b_{\alpha\beta}$ is the semi-minor axis of the elliptical equipotential lines and given by

$$2b_{\alpha\beta} = \sqrt{(\|d_{\alpha\beta}\| + \|d_{\alpha\beta} - y_{\alpha\beta}\|)^2 - \|y_{\alpha\beta}\|^2}, \quad (3)$$

where $y_{\alpha\beta} = (v_\beta - v_\alpha)\Delta t$ and $\Delta t = 0.5s$.

$$f_{\alpha\beta} = -\nabla_{d_{\alpha\beta}} V_{\alpha\beta}(b_{\alpha\beta}) = -\frac{dV_{\alpha\beta}(b_{\alpha\beta})}{db_{\alpha\beta}} \nabla_{d_{\alpha\beta}} b_{\alpha\beta}(d_{\alpha\beta}) \quad (4)$$

Equation 4 gives the repulsive force and $\nabla_{d_{\alpha\beta}}$ denotes the gradient with respect to distance between α and β. Using chain rule, this leads to

$$f_{\alpha\beta(d_{\alpha\beta})} = A_\alpha e^{-b_{\alpha\beta}/B} \cdot \frac{\|d_{\alpha\beta}\| + \|d_{\alpha\beta} - y_{\alpha\beta}\|}{2b_{\alpha\beta}} \cdot \frac{1}{2}\left(\frac{d_{\alpha\beta}}{\|d_{\alpha\beta}\|} + \frac{d_{\alpha\beta} - y_{\alpha\beta}}{\|d_{\alpha\beta} - y_{\alpha\beta}\|}\right). \quad (5)$$

Considering the angular dependence between two encountered visitors, with an angle of $\varphi_{\alpha\beta}$, the angular-dependent pre-factor $w(\varphi_{\alpha\beta})$ is given by the below

equations

$$\cos(\varphi_{\alpha\beta}) = \frac{v_\alpha}{||v_\alpha||} \cdot \frac{-d_{\alpha\beta}}{\|d_{\alpha\beta}\|} \quad (6)$$

$$w(\varphi_{\alpha\beta}(t)) = \left((1-\lambda_\alpha)\frac{1+\cos(\varphi_{\alpha\beta})}{2} + \lambda_\alpha\right), \quad (7)$$

where the parameter λ_α with $0 \leq \lambda_\alpha \leq 1$ is found by evolutionary optimization (details can be seen in [9]) as $\lambda_\alpha \approx 0.1$. The fitness of the social force model increases with the addition of the angular dependence formulation to the model.

As a consequence of SFM, the time it takes for the visitor to move to a destination point varies. The main impact of this model in the theme park scenario is that the usage of the same roads by the visitors causes an increase in the social interactions. This increase slows down the flow of the visitors along the roads. Since the theme parks are crowded areas with roads in which only pedestrian movements happen, the social force model is the best-fit model to represent the crowd dynamics and the micro-mobility behavior for the evacuation of the theme park visitors.

We illustrate the overall mobility behavior of a visitor according to the model in Fig. 3. Initially, the visitor starts with setting the target location by selecting the gate. After deciding the target location, the visitor tries to find waypoints in the visible local region and selects the best candidate if waypoints exist or sets a random point with the random exploration distance parameter. Micro-mobility phase, which is based on SFM, starts after deciding the next destination and ends whenever the visitor arrives the next destination. If the arrived location is not the target location, the movement continues by exploration of the local region, while in the case of reaching the target location, the visitors is marked as rescued.

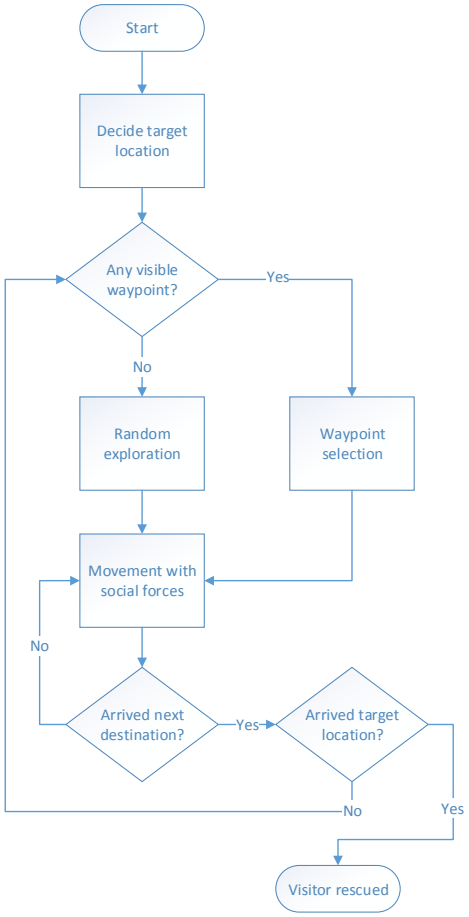

Fig. 3. Mobility behavior of a visitor during the simulation of the model.

III. Simulation Study

In this section, we discuss the evaluation of the mobility model. Our simulation study includes experiments and analysis from two simulations. The first is a mobility simulation in which we simulated the proposed mobility model along with other mobility models and compared with GPS traces of theme park visitors. We used the outcomes of the model for the simulation of an opportunistic network in which pedestrians carry mobile devices and evaluated performance of the network.

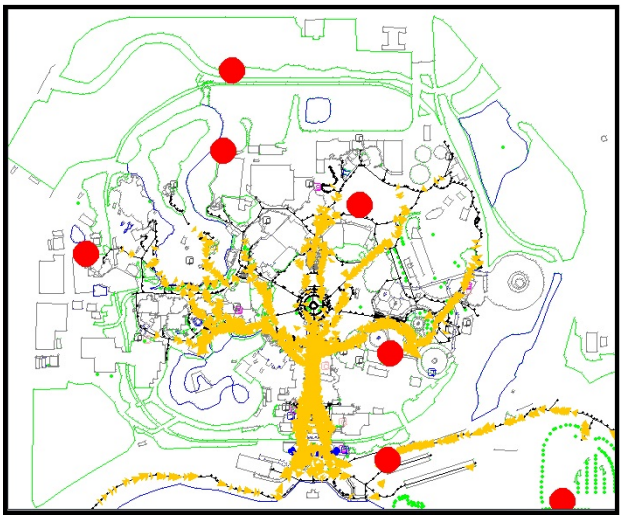

Fig. 4. The simulation of 2000 visitors and the impact of red zones in Magic Kingdom.

A. Mobility simulation setup

There are several mobility metrics used in the literature. These metrics can be classified in three types:

movement-based, link-based, and network-based metrics. In the mobility simulation, we focus on the movement- and the link-based metrics. The movement-based metrics are usually extracted from analyzing individuals' movement patterns. Flight lengths, average velocity, waiting times, mean-square distances are among the movement-based metrics. The link-based metrics analyze the effects of the mobility w.r.t. the relations between the mobile nodes such as their distances from each other. Average node density, variance of node density, average pairwise distances, relative mobility are examples of the link-based metrics.

The simulations of our model of theme park mobility for disaster scenarios (TP-D) are carried out to observe its characteristics. We then compare TP-D with the currently used mobility models and the 41 GPS traces (taken from the CRAWDAD archive at Darthmouth College) collected from 11 volunteers who spent their Thanksgiving or Christmas holidays at Disney World. The average duration of the mobility traces is approximately 9 hours with a minimum of 2.2 hours and maximum of 14.3 hours. The GPS tracking logs have a sampling time of 30 seconds. The traces are filtered in such a way that when a visitor is moving very fast, we assumed the visitor is in a vehicle traveling from one park to another. The remaining data is used for finding the set of flight lengths of each visitor where the flight length is defined as the distance between a pair of consecutive waypoints of a visitor.

The theme park mobility model (TP) [6] and self-similar least action human walk model (SLAW) [11] are used as realistic mobility models to simulate typical movement of theme park visitors. Random waypoint (RWP) model [12] is used as a generic model since it is the most commonly used mobility model in the network simulations. Simulations of these models run on 1000x1000 meters areas. Our goal is to gain insights about the mobility trajectories produced by the proposed TP-D model as opposed to these models. As these models do not support evacuation scenario, we do not aim to compare the success of these models.

Fig. 4 shows a snapshot from the simulation of 2000 visitors. The simulation of the model generates synthetic mobility traces of visitors in the terrain specified by the theme park map. The visitor in the theme park draws their trajectory lines while moving upon the waypoints with the goal of arriving at the gates. The dimension lengths of the maps vary from one park to another. For instance, the dimensions are close to 1000x1200 meters for Epcot and Magic Kingdom and approximately 650x750 meters for Islands of Adventure park of the Universal Studios. We used the theme park model of the Magic Kingdom in the experiments with 10000 visitors. We employ the circular specification of the SFM with the angular dependency using the same parameter values proposed in [9].

While we do not consider visitors whose escape time is more than 1000s as successfully evacuated, we include the output from all pedestrians in our averaged results such as the average evacuation times. Therefore, simulation time is empirically set to 2000s as in this duration almost all pedestrians achieve to arrive at their final destinations and consider the ones who may still stay in the disaster area as the outliers. Table I summarizes the default mobility simulation parameters and the parameters used for the SFM in the experiments.

TABLE I
MOBILITY SIMULATION PARAMETERS

simulation time	2000s
sampling time	10s
number of visitors	10000
min speed	0.0m/s
max speed	1.0m/s
number of red-zones	50
red-zone active time	1000s
red-zone radius	100m
random move distance	10m
max visibility	100m
wireless communication range	40m
SFM - interaction strength (A)	0.11 ± 0.06
SFM - interaction range (B)	0.84 ± 0.63
SFM - relaxation time (τ)	0.5s
SFM - λ	0.1

The simulation parameter values may differ due to various types of natural and man-made disasters occurring in different outdoor environments. For instance, disaster simulation experiments can be conducted using different *active time* of disaster events and *visibility* parameters. Based on the expected number of people and the possible types of disasters in certain environments, operators can run the mobility simulations with realistic parameter value ranges. In this simulation study, we focus on the mobility during a disaster in a theme park as an example disaster scenario.

B. Experimental results of the mobility model

1) Movement-based analysis: We start our evaluation with *flight lengths* which is one of the key properties of human mobility. A flight length is the distance between

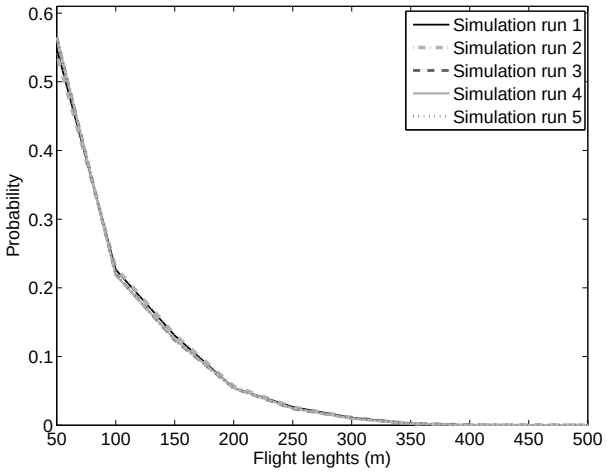

Fig. 5. Flight lengths probability distributions of TP-D for 5 simulation runs.

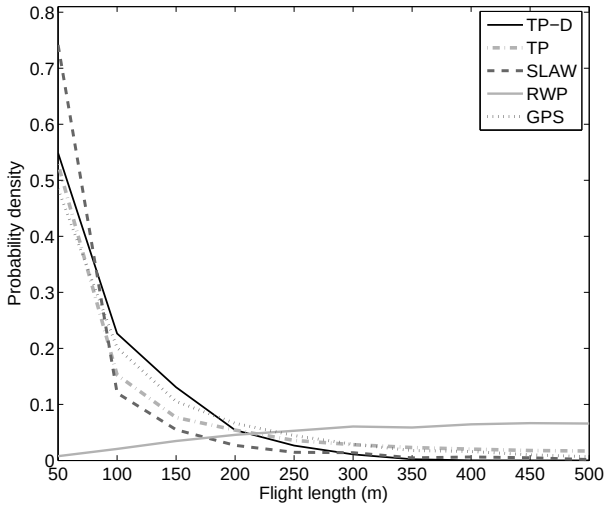

Fig. 6. Flight length probability distributions of TP-D, TP, SLAW, RWP, and the GPS traces.

a pair of consecutive pause points of a visitor in its trajectory. Mean, variance, and standard deviations of flight lengths are important statistical characteristics to observe diffusion characteristics [13] and characterize the human mobility patterns [14], [15]. The metric can be used for analyzing human mobility [16] in various scenarios including mobility during disaster [17] and theme park mobility [13], [18]. In our previous study [7], we analyzed the flight lengths based on the distance between waypoints in which a visitor decide the next destinations. In this analysis, however, instead of using waypoints on the map, the slowdown locations of the visitors are generated when they move less than 5m radius for more than 10s duration.

We first simulate flight length distributions of the TP-D model. We observed that the results of the simulation of the model for different simulation runs are almost identical, which shows the overall consistency of the simulation. Fig. 5 shows this consistency for the probability distribution function (PDF) of flight lengths among the 5 simulation runs which are randomly selected from a set of simulation runs having the same parameter settings. Moreover, Fig. 5 reveals that more than 50% of all flights are shorter than or equal to 50m and more than 20% are shorter than or equal to 100m. Hence, we observe a shorter flights due to frequent waiting in the pedestrian traffic caused by 10000 visitors.

We compared the flight length values of TP-D with TP, SLAW, RWP and the GPS traces. Fig. 6 shows PDF of flight lengths. We observed that the TP-D model produced shorter flight lengths compared to the TP model and the GPS traces. The SLAW model produced the shortest flight lengths due to the high density of fractal points used as waypoints of the simulation. However, the TP-D model produces outcomes closer to TP and the GPS traces. Being a mobility model which is specific to evacuation situation of disasters, TP-D interestingly has a similar flight length distribution. Moreover, all three models (TP-D, TP, SLAW) and the GPS traces have mostly lower than 200m flight lengths. On the other hand, RWP produces dramatically longer flight lengths with an average flight length of 500m and it can be classified as the most unrealistic model among the 4 models due to its significant mismatch with the GPS traces. While the default parameters of SLAW is used, output of the model is dependent on the number of fractal points created in the simulation area.

The mean values of the flight lengths with variations are shown in Fig. 7. The mean flight length value and the variation of TP-D is lower than TP and the GPS traces and higher than SLAW. Considering the difference between the ordinary movement of a visitor for the model TP and the GPS traces, flight lengths vary with the choices of the visitors such as visiting an attraction or going to the nearest restaurant. On the other hand, for the disaster scenario, the visitor has the only goal of moving towards the target locations as much as possible with the traffic. Due to the lack of choices and the similar traffics in the crowd flows of different roads, the lower variability with shorter flights is an expected outcome of the TP-D model.

2) Link-based analysis: Node degree of a pedestrian is defined as the number of neighbor pedestrians. The neighbors of the pedestrian are the ones who are in the communication range with the pedestrian. In other

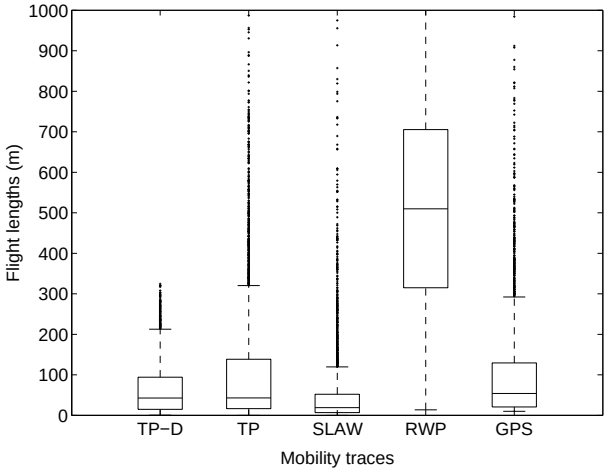

Fig. 7. Mean values of variations of flight length results of TP-D, TP, SLAW, RWP, and the GPS traces.

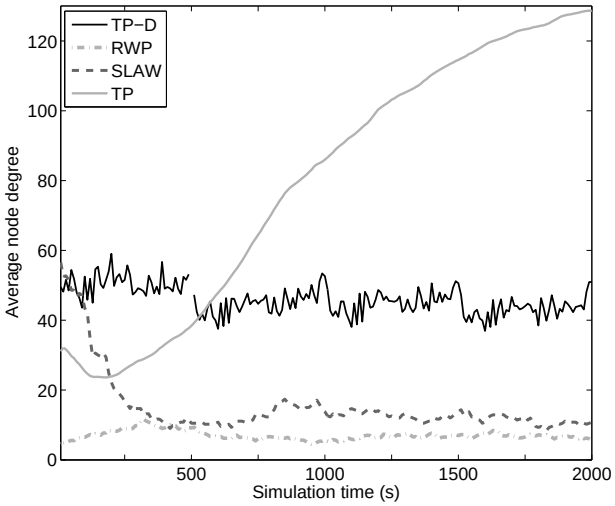

Fig. 8. Average node degrees by simulation time for TP-D, TP, SLAW, RWP, and the GPS traces.

words, two neighbors are assumed to have a wireless communication link between them if they are in the communication range of each other. Average node degrees is a link-based metric calculated as the average of the results of all pedestrians. Instead of comparing each individuals' node degrees, we observe the effects of mobility on the overall average by simulation time. Basically, a higher average node degree yields a better network performance. We assumed a transmission range of 40m. To be consistent in the comparison of average node degrees, the results are normalized to 1000 visitors in each model.

Fig. 8 shows the average node degrees by the simulation time for TP-D, SLAW, TP, and RWP. All mobility

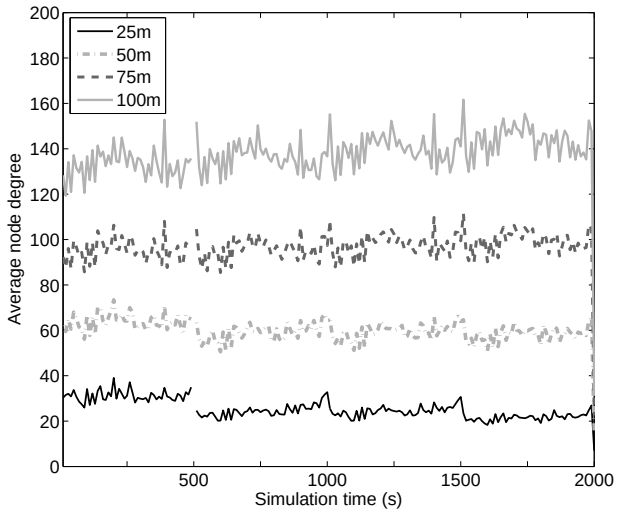

Fig. 9. Average node degrees by simulation time for transmissions ranges 25m, 50m, 75m, and 100m.

models generate distinct characteristic changes in node degrees with respect to the simulation time. TP-D has the highest average node degree along with SLAW at the initial phase since the mobile nodes are the initially distributed only on top of the roads while other models distribute the visitors to the entire area. We also see that the average node degrees stay close to the same level without a significant change, while the values may vary in short period of times. The main reason of the significant increase in node degrees in the TP model is the gathering behavior of visitors in the attractions. In TP, visitors start waiting in the queues very close to each other and therefore we see higher average node degrees after 2000s. In TP-D, however, pedestrians travel along the roads together, which do not produce the effect of the gathering behavior. SLAW model has an initial phase of 500s and the results converges to a constant level. While the gathering behavior of SLAW is not visible for 40m communication range, it may be observed for longer ranges. RWP stays constant with some variances in short times caused by the randomness.

We analyzed the average node degrees with various transmission ranges to see the possible effects of the mobility of the visitors on the performance of networks in various simulation times. Fig. 9 reveals that for various transmission ranges (25m, 50m, 75m and 100m), average node degree stays consistent throughout the simulation with the fluctuations which also exist in the previous results. Moreover, as an expected overall effect of the transmission range parameter, average node degrees increased for higher transmission range values.

The distances between all pairs of mobile nodes are

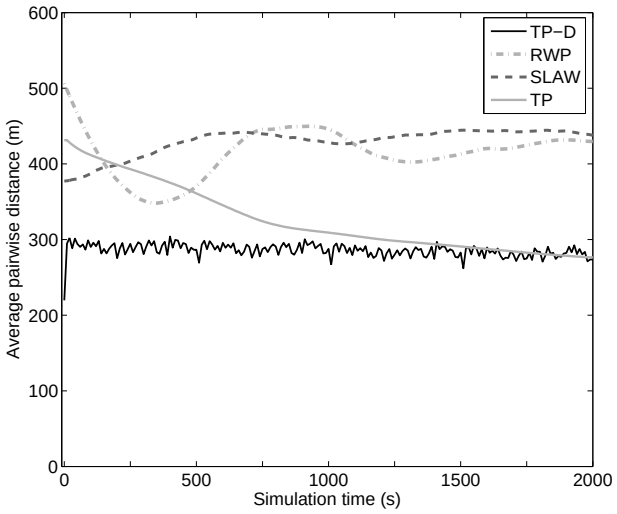

Fig. 10. Average pairwise distances by simulation time for TP-D, TP, SLAW, RWP, and the GPS traces.

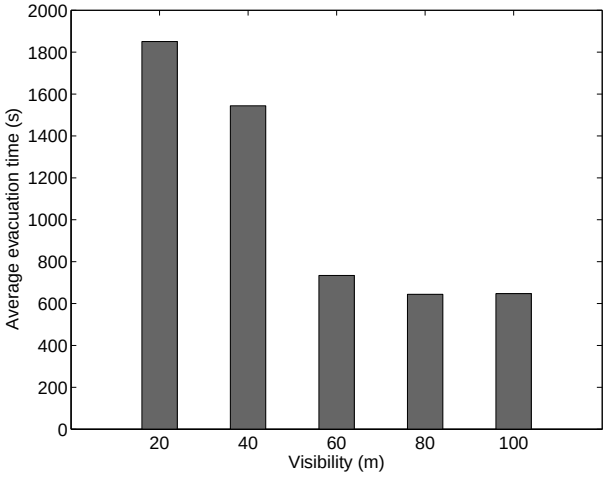

Fig. 11. Effects of the visibility on evacuation times.

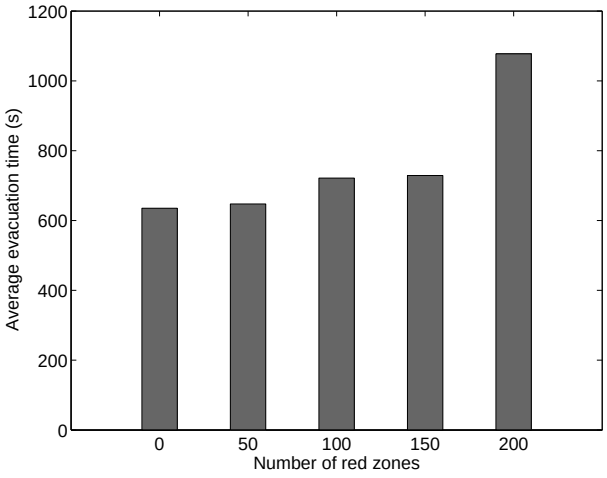

Fig. 12. Effects of the number of red-zones on evacuation times.

averaged to calculate average pairwise distances. As a link-based metric, average pairwise distance helps us to evaluate the closeness of a node to another on average. This metric shows the possibility to form a new network with a desired subset of all the mobile nodes. Smaller pairwise distances are expected for better network performances. As in the average node degree results, we observed the effects of the mobility on the results by simulation times.

As it can be seen in Fig. 10, all the models again have distinct characteristics. TP-D has a consistency with a small overall constant decay of average pairwise distances. As also observed in the previous experiment, the pedestrians becomes closer to each other as the time passes. An interesting difference of this experiment compared to the previous one is that the significance of the change in the results of TP becomes weaker.

For instance, when a visitor goes to an attraction, the pairwise distance with the other visitors in the same attraction becomes smaller, while the visitor's pairwise distance with the rest of the crowd in other attractions of the park may become larger. In TP-D, on the other hand, people mostly move towards the similar target locations. Furthermore, since we consider the pedestrians who reached the exit gates as removed and do not take them into consideration, quick increase due to the gathering behavior does not exist in TP-D. After the initial phase of 500s, SLAW and RWP models reach steady-states having constant average pairwise distances with some variances due to randomness in the models.

3) Evacuation performance: Evacuation time is the time it takes for the visitors to reach the target (exit) points from the beginning of the simulation. The results of the evacuation times are analyzed for various values of the visibility and the number of red-zones parameters. The simulations of TP, SLAW and RWP are not used for analysis, since these models do not involve the evacuation of the environment.

In order to see the impact of the local knowledge, we compare the TP-D model with various maximum visibility values. We see in Fig. 11 that the increase in the visibility causes an overall decrease in evacuation times as expected. However, after the maximum visibility value of 80 meters, this effect loses its significance.

As shown in Fig. 12, we observed the relation between the number of red-zones and the evacuation times. The higher numbers of red-zones constantly produce the higher evacuation times, which is an expected negative

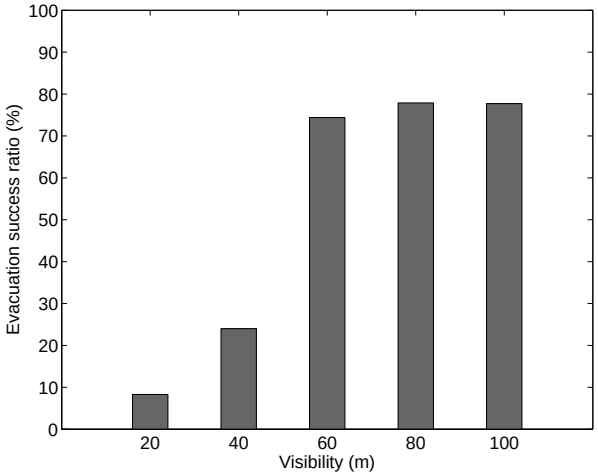

Fig. 13. Effects of the visibility on evacuation success ratio.

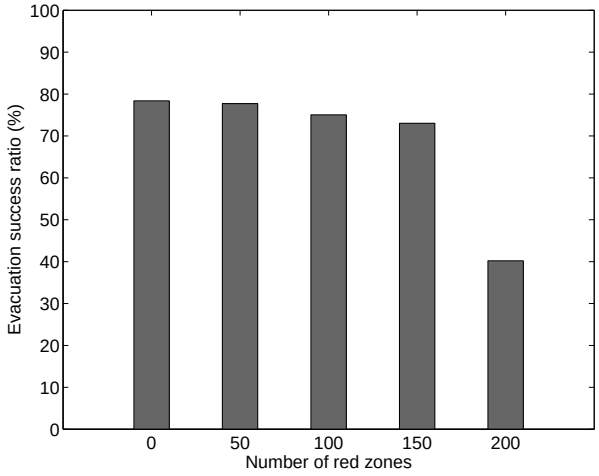

Fig. 14. Effects of the number of red-zones on evacuation success ratio.

effect of the red-zones. The reason behind this negative effect can be easily observed by looking at the snapshot of the visitor flows in Fig. 4. Among the 7 currently active red-zones which are randomly positioned, 2 of them are located in a way that they prevent the regular flow of the visitors. This impact of preventing the visitors from moving along the road and tunneling them to other ways is the reason for the increase in the average evacuation times. Since red-zones are generated at random regions of the map, in some simulation runs red-zones happen to occur on top of the roads and therefore produce significantly higher evacuation times as in the 200 red-zones example shown in Fig 12.

We define the evacuation success ratio as the ratio of the number of visitors who were evacuated in less than a specified time limit. We assume that the visitors who could not reach the gates in the acceptable time are not successfully evacuated. We set the time limit as 1000s and analyze the evacuation success ratio according to the visibility and number of red-zones parameters.

Fig. 13 shows the evacuation success ratios with visibility ranging from 20m to 100m. As it can be seen in the figure, increased visibility produce higher evacuation success ratios. Specifically, from 20m to 40m, the success ratio increases more than two times and the maximum visibility value of 60m allows the dynamic flow of the visitors with a 75% success ratio. The significance of the increase decreases dramatically for values higher than 60m. Because of the fact that visibility plays an important role in the evacuation time and success ratio, the parameter should be set according to the specific simulated disaster. While the limitation caused by various types of disasters in the vision of pedestrians is not within the scope of this study, this should be further investigated for realistic simulations.

Fig. 13 shows the evacuation success ratios with no red-zone and red-zone ranging from 50 to 200. The success ratio drops from approximately 80% to 40% with 200 red-zones compared to the 0 red-zone which is the case of no direct disaster impact in any region of the theme park. Again, due to the occurrence of the red-zones on the roads, 200 red-zones produced significantly lower success ratios, while 150 red-zones have more than 70% evacuation success ratio.

C. Network simulation setup

We include the network simulation results to show a practical application of our disaster mobility model. The mobility model can be used to evaluate success of different network models and various disaster management strategies such as using trained personnel to assist the visitors for faster evacuation during or before disasters.

In this section, we discuss the effects of the TP-D mobility model on the performance of an opportunistic network with mobile sinks. As a disaster response strategy, mobile sinks are used for search and rescue operations and tracking the theme park pedestrians during their evacuation. In this experiment mobile sinks broadcast a message to sensor nodes using epidemic routing and mark the sensor nodes as detected if they send acknowledgment. For the application scenario of theme park visitors carrying smartphones as sensor devices and sending message in need of a rescue and a limited number of mobile sinks, we analyze the network coverage and rescue success performances.

The network model is previously proposed [19] with the three mobile sink modalities: “physical force-based”

(PF), "grid allocation-based" (GA) and "road allocation-based" (RA). In PF, mobile sinks position themselves according to gravitational forces from sensor devices and mobile sinks. Sensor devices have a pulling force while sinks have a pushing force on each other. In GA, the roads in the theme park map is divided into grids and each sink is given a close to even number of grids for patrolling. In RA, the mobile sinks share the available roads for patrolling. We also included two random sink mobility models for comparison, which we call "random target location" (RTL) and "random waypoint distribution" (RWD) models. In RTL, each sink chooses any random target location on the map, then sets the closest waypoint to the location as the sink's next destination. In RWD, each sink chooses a waypoint randomly among all waypoints as the next destination. RWD favors the popular roads because popular roads tend to include more waypoints than the other roads.

The network performance-based metrics show the effects of the mobility on the performance of the network. Unlike the movement-based and link-based metrics, the results with network-based metrics depend on not only the movement of the mobile nodes, but also the network model. For instance, along with the movements of the mobile nodes, the transmission range and protocols for routing and transmission scheduling affect the results. We analyzed transmission counts, number of detected sensors, recontact rates and rescue success ratios in order to observe the network coverage and energy efficiency results according to the chosen sink mobility models.

We evaluated the success of a network with varying mobile sinks from 1 to 10 and transmission ranges 10m through 100m to analyze the effects of available resources. Evaluation of each setting is based on 50 simulation runs. Each simulation run generates at least 2000 message transmissions among sensor nodes or with mobile sinks, while the number of transmissions to the mobile sinks varies because of the sink mobility model selection and parameters such as the number of mobile sinks. The wireless transmissions between the sensor nodes and from the sensor nodes to the mobile sinks are based on the epidemic routing protocol [20].

Table I includes the list of the simulation parameters.

Disasters tend to have effects on the random locations of the area during the simulation time. In the network simulation, instead of creating artificial disaster zones, we marked the pedestrians effected by the disaster.

D. Opportunistic network performance

We start analyzing the network performance with the number of transmissions occurred among all the pairs during the simulation. A pair may include either two sensor nodes or a sensor node and a mobile sink and each session includes 3 message transmissions. We consider average number of transmissions of all nodes in the network including the transmissions in successful or failed sessions. For the number of transmissions metric, there is a tradeoff such that higher number of message transmissions may cause excessive energy consumption while lower number of transmissions may be a result of unsuccessful network coverage.

Fig. 15 shows the results of the approaches with 5 mobile sinks for transmission ranges of 10m, 25m, 50m and 100m. First of all, we observed that increase in transmission range dramatically increases the number of transmissions. This is an expected result caused by the exponential increase in the number of neighbors of a sensor node. In the case of having limited energy resources, a more effective routing protocol may provide better energy preservation for sensor nodes with high transmission ranges. Secondly, since the sinks are in limited number compared to 200 sensor nodes, the effect of the mobile sink mobility is not very significant. Even

TABLE II
SIMULATION PARAMETERS

number of sensor nodes	200
sensing range	20 m
sensor message storage capacity	100
transmission probability	0.9
number of effected people	20
rescue failure time	600 s
mobile sink max speed	1 m/s

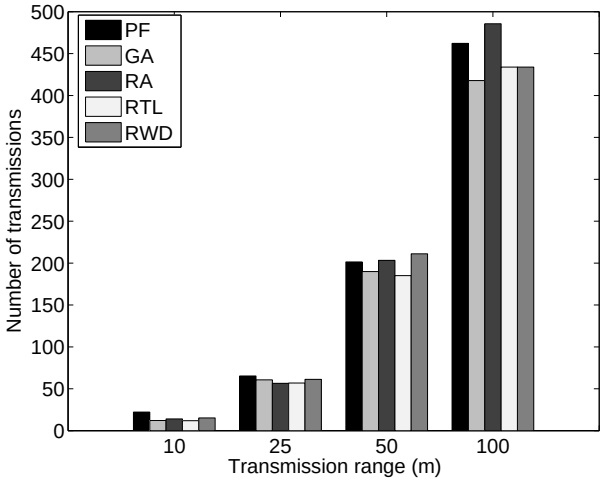

Fig. 15. Number of transmissions of PF, GA, RA, RTL and RWD for 10m, 25m, 50m and 100m transmission ranges.

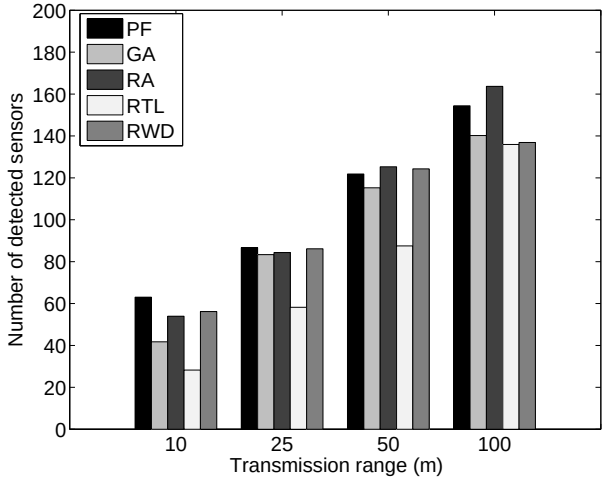

Fig. 16. Number of detected sensors of PF, GA, RA, RTL and RWD for 10m, 25m, 50m and 100m transmission ranges.

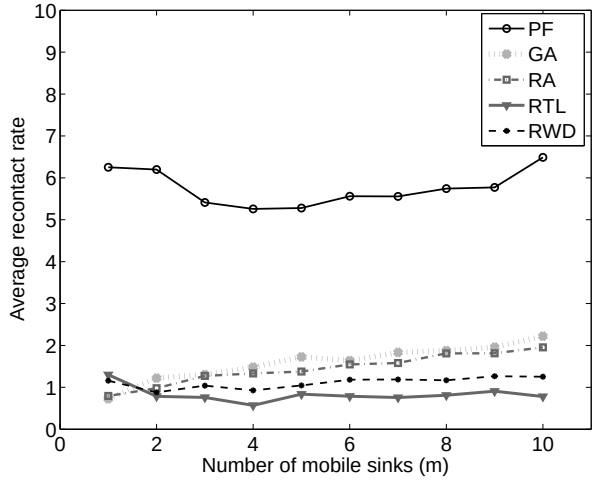

Fig. 17. Recontact rates of PF, GA, RA, RTL and RWD for 1 to 10 sinks.

though the number of sensor nodes are only 10% of all 2000 visitors, the sensor nodes are highly active for transmission range of 50m. Each sensor node has on average approximately 200 transmissions occurred during the pedestrian's walk to target point. While 100m transmission range produces significantly higher number of transmissions, it may cause an excessive energy consumption due to wireless communication.

During the simulation time of the network, mobile sinks have direct encounter with some of the sensor nodes such that the distance between them is less than the transmission range. In this case, we count the sensor device as a detected device and define the number of detected sensors as a network coverage metric.

Fig. 16 reveals the number of detected sensor for transmission ranges of 10m, 25m, 50m and 100m. Among all the approaches, RA and PF are the overall winners reaching up to more than 80% of the 200 sensor nodes. RWD also provides a reasonably good coverage of sensor nodes since the mobile sinks mostly choose the popular locations where sensor nodes are also most likely present. With higher transmission ranges, the coverage performance is better for all the approaches. Most sink mobility approaches provide an acceptable coverage with 50m or 100m transmission range such that most sensors have direct encounter with at least one mobile sink along their way.

We analyzed the recontact count for each pair of sink and sensor node, which is the number of contacts of the mobile sink and the sensor node after their first communication. Recontact rate of a mobile sink is its average recontact count with all the sensor nodes. Fig. 17 shows the results of average recontact rates for

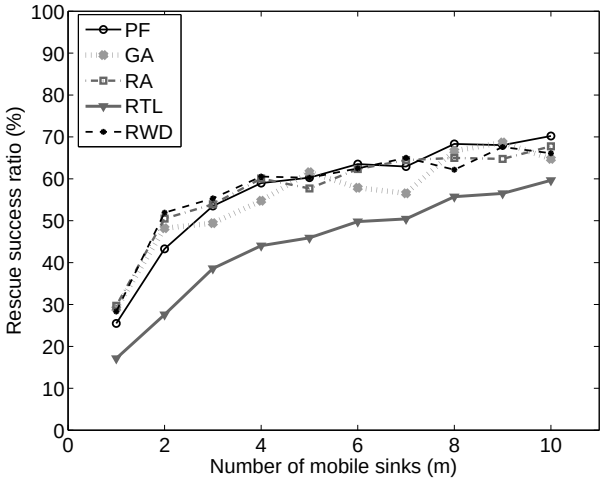

Fig. 18. Rescue success ratios of PF, GA, RA, RTL and RWD for 1 to 10 mobile sinks.

simulation settings with 1 to 10 sinks. PF outperforms others with an average rate of more than 5.0 due to sinks' behavior of following sensor nodes and keeping in touch as much as possible.

For the setting with only 1 mobile sink, we observed that recontact rates of GA, RA, RTL and RWD are low without any significant difference between them, while the rate difference becomes significant with multiple sinks.

In the case of emergency events during disasters such as visitors in need of urgent help, the mobile sinks should be able to reach the regions of these events as quick as possible. For the successful event coverage, we consider the maximum acceptable time for a mobile sink to arrive to an emergency event region as the *r*escue time.

We observed the message delay, the time it takes for the sink after receiving a message to reach the effected pedestrians. We assume a rescue time of 10 minutes, which includes the message delay and the travel time of the mobile sink. Fig. 18 shows the rescue success ratio with respect to varying the number of mobile sinks with the transmission range of 25m. With 10 mobile sinks, PF reaches more than 70% of an effected pedestrian in less than 10 minutes. For RTL, success ratio increases from 10% to 60% from 1 to 10 mobile sinks while for the other approaches it increases approximately from 30% to 70%.

Overall, the network simulation study provides promising results for disaster scenarios in theme parks in terms of opportunistic communication with the use of 200 mobile devices, which corresponds to participation of only 2% of the 10,000 visitors. Moreover, limited number of mobile sinks can be used to track the visitors carrying mobile devices and rescue them if needed. Higher rescue success ratios can be achieved with higher speed vehicles. A possible real-world implementation of a mobile sink can be a rescue robot or a security guard driving a personal electric transportation vehicle (e.g. Segway Patroller [21]) with a tablet computer.

IV. Related Work

In this section, we summarize the related work for the mobility models and studies of disaster mobility and management.

A. Mobility models

González et al. [14] analyze the trajectory of 100,000 mobile phone users for a time period of six months and find that the trajectories have a high degree of temporal and spatial regularity. While commercial telecom networks do not track movement patterns of every mobile user, Lin et al. [22] propose the use of standard outputs from cell phones such as handover rates, call arrival rates, call holding time, and call traffic to investigate human movement patterns. Social force model [9] is proposed by Helbing and Johansson to represent the micro-mobility behavior of the pedestrians in crowded areas. Helbing [23] also studied evacuation problem and disasters mobility [24]. Song et al. [25] analyzed the mobile phone users trajectories and found 93% potential predictability in mobility of the users. De Domenico et al. [26] consider movements of friends and their correlated mobility patterns by their social interactions for predicting human mobility.

Munjal et al. [27] review the changing trends of mobility models used for simulations of opportunistic communication networks. They offer use of mobility models based on real data or well-known features of human movement decisions, instead of random mobility models. They also list challenges for future research of human mobility. Wu et al. [28] propose a technique to improve the accuracy of global positioning with the help of human mobility. A cooperative sensing framework is proposed for mobile opportunistic networks by Zhao et al. [29]. The performance of their proposed data forwarding schemes, namely Epidemic Routing with Fusion (ERF) and Binary Spray-and-Wait with Fusion (BSWF), rely on the human mobility as well as vehicle mobility in various scenarios. Wu et al. [30] proposed opportunistic data collection by leveraging human mobility as they carry smartphones.

Self-Similar Least-Action Walk (SLAW) [11] is a generic human walk model which produces synthetic mobility traces. These traces have certain statistical characteristics of human mobility. These five characteristics are listed as: 1) flight lengths and pause times with heavy-tail distribution, 2) heterogeneously bounded movement regions, 3) truncated power-law ICTs, 4) self-similarity, and 5) least-action trip planning. SLAW tries to emulate individual mobility and each individual's movement is independent from each other, assuming that they do not have any social interactions. SLAW model uses self-similar waypoints which are generated over a 2D plane. As the gaps between the waypoints determine the flight lengths, Hurst parameter (H) of self-similar points controls the gap distribution characteristics. The waypoints are clustered and each individual randomly chooses a cluster as the movement region for a daily trip. Each individual starts their walk by randomly choosing a waypoint as the starting point and later makes movement decisions based on the least-action trip planning (LATP) algorithm. In LATP, a person decides the next destination by selecting a waypoint in the cluster and straightly moves to that destination. The equation in LATP algorithm for assigning probability values for deciding the next destination waypoints is given as follows.

$$P(w) = \frac{d(v,w)^{-\alpha}}{\sum_{w_i \in W - W'} d(v,w_i)^{-\alpha}}, \tag{8}$$

where $P(w)$ is the probability of visiting the next destination waypoint w ($w \in W - W'$), v is the waypoint on top of which the person is currently waiting, and $d(v,w)$ is the Euclidean distance between the two waypoints. W is set of the waypoints which are planned to be visited and W' is the set of already visited waypoints. The value of the parameter α is set according to the GPS traces collected from the specific outdoor environment

for providing statistical match. For instance, $\alpha = 3$ produces the difference less than only 2% between the synthetic mobility traces and the GPS traces for Disney World. LATP is shown to produce mobility traces that matches the real GPS traces very well for the range $1 \leq \alpha \leq 3$.

Munjal et al. [31] propose a simple mobility model, SMOOTH, that represents the similar characteristics of SLAW. Schwamborn and Aschenbruck [32] extend the SLAW with their Map-based SLAW (MSLAW) model which takes the effects of the geographical restrictions into account for human walks. Vukadinovic et al. [33] propose a simple framework to simulate mobility of theme park visitors. They use OSM for generation of maps and calibrate the framework parameters according to the GPS traces. ParkSim [34] by Vukadinovic et al. is a software tool simulating the mobility of theme park visitors. The mobility model of ParkSim is driven by the possible activities of the visitors in the park. Mei and Stefa [35] propose SWIM, a simple mobility model which generates synthetic mobility traces for ad hoc networking and Papageorgiou et al. [36] propose a human mobility model considering obstacles as the integral part of the areas and study the properties of the resulting network topologies. Our mobility model differs with the previously mentioned models as it simulates the mobility of visitors during evacuation in disaster scenarios.

A variety of mobility models have been proposed for simulating specific-scenarios. Liu et al. [37] propose a physics-based model of skier mobility in mountainous regions by considering the physical effects of gravity and the steepness of the terrain. The goal of the model is to evaluate the effectiveness of wireless communication devices in improving avalanche safety. Hsu et al. [38] propose the Weighted Waypoint Mobility model for the pedestrian mobility inside campus environments. Kim et al. [39] propose a mobility model for urban wireless networks, in which the model parameters are derived from urban planning surveys and traffic engineering research. Helgason et al. [40] investigate the effects of the human mobility on the wireless communication performance of ad hoc and delay tolerant networks.

B. Disaster mobility and management

There exist various studies related to disaster management. Winter et al. [41] study the evacuation problem in disaster areas and propose the use of a mobile service "Get-Me-Out-Of-Here" (GOH) running on smartphones. Benefits of communication among people are observed for the evacuation scenarios in which individuals have only the local knowledge of the environment. Uddin et al. [42] propose an agent-based mobility model for the mobility of people with different roles such as rescue workers and volunteers as well as vehicles such as police patrol cars and ambulances. They also propose the intercontact routing [43] for disruption-tolerant disaster response networks to reduce the resource overhead. Zheng et al. [44] propose a disaster management system framework based on data mining and information retrieval techniques for disaster preparedness and recovery.

Patrix et al. [45] model mobility of agents and disaster area for crowd behavior detection. In this study, they model obstacles, dangers, and shelters as separate zones in their simulation of the disaster scenario. An agent makes movement decisions according to these zones and the movement of the other agents. A role-based mobility model is proposed by Nelson et al. [46] for disaster areas. In this model, movement patterns of objects with distinct roles such as police and civilians differ according to their various reactions to the events. Aschenbruck et al. [47] propose a heterogeneous area-based movement of different roles, such as vehicles and firefighters. They separate the disaster area in various sub-areas such as incident site, casualties treatment area, transport zone, and hospital zone. Bagrow et al. [48] study collective response behavior and changes in communications of people in extreme emergency conditions such as bombing, plane crash, earthquake and power blackout. Patterson et al. [49] highlight models which focus on the effects of communities on preparedness, response, and recovery of people from disasters. Kirchhoff et al. [50] propose link quality based routing, prioritization of control messages, and overhead reduction mechanisms for mobile wireless multi-hop networks. These mechanisms are useful for disaster scenarios with major challenges such as limited network capacity and link variability. Song et al. [51] propose a disaster mobility model based on the earthquakes occured in Japan over 4 years period. Their human mobility dataset includes GPS measurements from 1.6 million people. These GPS measurements can be seen as the products of the transportation services in Tokyo. Our model differs from the above models such that we focus on modeling human mobility in disaster areas by isolating it from other challenges such as transportation or security.

V. Conclusion

In this paper, we studied pedestrian mobility for disaster areas. We considered the application scenario of theme parks and proposed the theme park disaster (TP-D) mobility model. We used real theme park maps to model the environment. The mobility of theme park

visitors are modeled by the theme park models and the social force model. We analyzed the outcomes of the simulation of our model in comparison with the simulations of currently used models and the GPS traces of theme park visitors. Using our mobility model, we evaluated the success of an opportunistic communication network with mobile sinks.

The proposed mobility model can be used for evaluating new disaster response strategies and various network models for use in theme park environments. Moreover, the techniques used for developing our mobility model of theme park visitors can be applied for modeling human mobility in other environments such as university campuses and shopping plazas.

VI. Acknowledgment

We thank Prof. George Kesidis from The Pennsylvania State University for his valuable discussion of mobility models with our research group which led to the study of the evacuation problem in disaster areas. We also acknowledge the use of human mobility traces from the CRAWDAD archive at Dartmouth College.

References

[1] T. Camp, J. Boleng, and V. Davies, "A survey of mobility models for ad hoc network research," *Wireless Communications and Mobile Computing*, vol. 2, no. 5, pp. 483–502, September 2002.

[2] D. Karamshuk, C. Boldrini, M. Conti, and A. Passarella, "Spot: Representing the social, spatial, and temporal dimensions of human mobility with a unifying framework," *Pervasive and Mobile Computing*, vol. 11, pp. 19–40, 2014.

[3] "Theme index: Global attractions attendance report," Themed Entertainment Association (TEA), Tech. Rep., 2013.

[4] M. K. Van Aalst, "The impacts of climate change on the risk of natural disasters," *Disasters*, vol. 30, no. 1, pp. 5–18, 2006.

[5] A. S. Cacciapuoti, F. Calabrese, M. Caleffi, G. Di Lorenzo, and L. Paura, "Human-mobility enabled wireless networks for emergency communications during special events," *Pervasive and Mobile Computing*, vol. 9, no. 4, pp. 472–483, 2013.

[6] G. Solmaz, M. Akbas, and D. Turgut, "A mobility model of theme park visitors," *IEEE Transactions on Mobile Computing*, vol. 14, no. 12, pp. 2406–2418, December 2015.

[7] G. Solmaz and D. Turgut, "Theme park mobility in disaster scenarios," in *Proc. of the IEEE GLOBECOM'13*, December 2013, pp. 377–382.

[8] G. Solmaz and D. Turgut, "Pedestrian mobility in theme park disasters," *IEEE Communications Magazine*, vol. 53, no. 7, pp. 172–177, July 2015.

[9] D. Helbing and A. Johansson, "Pedestrian, crowd and evacuation dynamics," *Encyclopedia of Complexity and Systems Science*, vol. 16, no. 4, pp. 6476–6495, 2010.

[10] M. Haklay and P. Weber, "OpenStreetMap: User-generated street maps." *Pervasive Computing*, vol. 7, no. 4, pp. 12–18, December 2008.

[11] K. Lee, S. Hong, S. J. Kim, I. Rhee, and S. Chong, "SLAW: self-similar least-action human walk," *IEEE/ACM Transactions on Networking*, vol. 20, no. 2, pp. 515–529, April 2012.

[12] J. Broch, D. A. Maltz, D. B. Johnson, Y.-C. Hu, and J. Jetcheva, "A performance comparison of multi-hop wireless ad hoc network routing protocols," in *Proc. of the MobiCom'98*, October 1998, pp. 85–97.

[13] I. Rhee, M. Shin, S. Hong, K. Lee, S. J. Kim, and S. Chong, "On the Lévy-walk nature of human mobility," *IEEE/ACM Transactions on Networking*, vol. 19, no. 3, pp. 630–643, June 2011.

[14] M. C. González, C. A. Hidalgo, and A.-L. Barabási, "Understanding individual human mobility patterns," *Nature*, vol. 453, no. 7196, pp. 779–782, 2008.

[15] B. Jiang, J. Yin, and S. Zhao, "Characterizing the human mobility pattern in a large street network," *Physical Review E*, vol. 80, no. 2, p. 021136, 2009.

[16] M. Khaledi, H. R. Rabiee, and M. Khaledi, "Fuzzy mobility analyzer: A framework for evaluating mobility models in mobile ad-hoc networks," in *Wireless Communications and Networking Conference (WCNC), 2010 IEEE*. IEEE, 2010, pp. 1–6.

[17] S. Pomportes, J. Tomasik, and V. Vèque, "A composite mobility model for ad hoc networks in disaster areas," *REV Journal on Electronics and Communications*, vol. 1, no. 1, 2011.

[18] G. Solmaz, M. İ. Akbaş, and D. Turgut, "A mobility model of theme park visitors," *IEEE Transactions on Mobile Computing*, vol. 14, no. 12, pp. 2406–2418, 2015.

[19] G. Solmaz and D. Turgut, "Tracking evacuation of pedestrians during disasters," in *Proc. of IEEE GLOBECOM'15*, December 2015.

[20] A. Vahdat and D. Becker, "Epidemic routing for partially connected ad hoc networks," Technical Report CS-200006, Duke University, Tech. Rep., 2000.

[21] "SEGWAY," http://www.segway.com.

[22] Y.-B. Lin, C.-C. Huang-Fu, and N. Alrajeh, "Predicting human movement based on telecom's handoff in mobile networks," *IEEE Transactions on Mobile Computing*, vol. 12, no. 6, pp. 1236–1241, 2013.

[23] D. Helbing, "Simulation of pedestrian crowds in normal and evacuation situations," *Most*, vol. 21, pp. 21–58, 2002.

[24] M. Moussaïd, D. Helbing, and G. Theraulaz, "How simple rules determine pedestrian behavior and crowd disasters," *Proc. of the National Academy of Sciences*, vol. 108, no. 17, pp. 6884–6888, 2011.

[25] C. Song, Z. Qu, N. Blumm, and A.-L. Barabsi, "Limits of predictability in human mobility," *Science*, vol. 327, no. 5968, pp. 1018–1021, February 2010.

[26] M. De Domenico, A. Lima, and M. Musolesi, "Interdependence and predictability of human mobility and social interactions," *Pervasive and Mobile Computing*, vol. 9, no. 6, pp. 798–807, 2013.

[27] A. Munjal, T. Camp, and N. Aschenbruck, "Changing trends in modeling mobility: a simple way to model human walks," *Journal of Electrical and Computer Engineering*, vol. 2012, pp. 1–16, October 2012.

[28] C. Wu, Z. Yang, Y. Xu, Y. Zhao, and Y. Liu, "Human mobility enhances global positioning accuracy for mobile phone localization," *IEEE Transactions on Parallel and Distributed Systems*, vol. 26, no. 1, pp. 131–141, Jan 2015.

[29] D. Zhao, H. Ma, S. Tang, and X.-Y. Li, "Coupon: A cooperative framework for building sensing maps in mobile opportunistic networks," *IEEE Transactions on Parallel and Distributed Systems*, vol. 26, no. 2, pp. 392–402, Feb 2015.

[30] X. Wu, K. N. Brown, and C. J. Sreenan, "Analysis of smartphone user mobility traces for opportunistic data collection in wireless sensor networks," *Pervasive and Mobile Computing*, vol. 9, no. 6, pp. 881–891, 2013.

[31] A. Munjal, T. Camp, and W. C. Navidi, "SMOOTH: a simple way to model human walks," *ACM SIGMOBILE Mobile Com-*

puting and Communications Review, vol. 14, no. 4, pp. 34–36, November 2010.

[32] M. Schwamborn and N. Aschenbruck, "Introducing geographic restrictions to the slaw human mobility model," in *Proc. of the IEEE MASCOTS'13*, Aug 2013, pp. 264–272.

[33] V. Vukadinovic, F. Dreier, and S. Mangold, "A simple framework to simulate the mobility and activity of theme park visitors," in *Proc. of the WSC'11*, December 2011, pp. 3248–3260.

[34] V. Vukadinovic, F. Dreier and S. Mangold, "Impact of human mobility on wireless ad hoc networking in entertainment parks," *Ad Hoc Networks*, June 2012.

[35] A. Mei and J. Stefa, "Swim: A simple model to generate small mobile worlds," in *Proc. of the IEEE INFOCOM'09*, April 2009, pp. 2106 –2113.

[36] C. Papageorgiou, K. Birkos, T. Dagiuklas, and S. Kotsopoulos, "An obstacle-aware human mobility model for ad hoc networks," in *Proc. of the IEEE MASCOTS '09*, Sept 2009, pp. 1–9.

[37] X. Liu, C. Williamson, and J. Rokne, "Physics-based modeling of skier mobility and avalanche rescue in mountainous terrain," in *Proc. of the IEEE LCN'10*, October 2010, pp. 645–652.

[38] W. Hsu, K. Merchant, H. Shu, C. Hsu, and A. Helmy, "Weighted waypoint mobility model and its impact on ad hoc networks," *ACM SIGMOBILE Mobile Computing and Communications Review*, vol. 9, no. 1, pp. 59–63, January 2005.

[39] J. Kim, V. Sridhara, and S. Bohacek, "Realistic mobility simulation of urban mesh networks," *Ad Hoc Networks*, vol. 7, no. 2, pp. 411–430, March 2009.

[40] Ó. Helgason, S. T. Kouyoumdjieva, and G. Karlsson, "Opportunistic communication and human mobility," *IEEE Transactions on Mobile Computing*, vol. 13, no. 7, pp. 1597–1610, 2014.

[41] S. Winter, K.-F. Richter, M. Shi, and H.-S. Gan, "Get me out of here: collaborative evacuation based on local knowledge," in *Proc. of the IWCTS'11*, November 2011, pp. 35–42.

[42] M. Uddin, D. Nicol, T. Abdelzaher, and R. Kravets, "A post-disaster mobility model for delay tolerant networking," in *Proc. of the WSC'09*, December 2009, pp. 2785 –2796.

[43] M. Uddin, H. Ahmadi, T. Abdelzaher, and R. Kravets, "Intercontact routing for energy constrained disaster response networks," *IEEE Transactions on Mobile Computing*, vol. 12, no. 10, pp. 1986–1998, Oct 2013.

[44] L. Zheng, C. Shen, L. Tang, C. Zeng, T. Li, S. Luis, and S.-C. Chen, "Data mining meets the needs of disaster information management," *IEEE Transactions on Human-Machine Systems*, vol. 43, no. 5, pp. 451–464, 2013.

[45] J. Patrix, A.-I. Mouaddib, and S. Gatepaille, "Detection of primitive collective behaviours in a crowd panic simulation based on multi-agent approach." *International Journal of Swarm Intelligence Research*, vol. 3, no. 3, pp. 50–65, June 2012.

[46] S. C. Nelson, A. F. Harris, III, and R. Kravets, "Event-driven, role-based mobility in disaster recovery networks," in *Proc. of the ACM CHANTS'07*, September 2007, pp. 27–34.

[47] N. Aschenbruck, E. Gerhards-Padilla, and P. Martini, "Modeling mobility in disaster area scenarios," *Performance Evaluation*, vol. 66, no. 12, pp. 773–790, 2009.

[48] A.-L. B. James P. Bagrow, Dashun Wang, "Collective response of human populations to large-scale emergencies," *PLoS ONE*, vol. 6, no. 3, March 2011.

[49] O. Patterson, F. Weil, and K. Patel, "The role of community in disaster response: Conceptual models," *Population Research and Policy Review*, vol. 29, no. 2, pp. 127–141, April 2010.

[50] J. Kirchhoff, J. Bauer, R. Ernst, C. Fuchs, S. Jopen, and N. Aschenbruck, "Extending odmrp for on-site deployments in disaster area scenarios," in *Proc. of the IEEE IPCCC'13*, December 2013, pp. 1–10.

[51] X. Song, Q. Zhang, Y. Sekimoto, R. Shibasaki, N. J. Yuan, and X. Xie, "Prediction and simulation of human mobility following natural disasters," *ACM Transactions on Intelligent Systems and Technology (TIST)*, vol. 8, no. 2, p. 29, 2016.